Acta Neuropathol (1998) 96 : 401–408

REGULAR PAPER

T. Komori · N. Arai · M. Oda · H. Nakayama
H. Mori · S. Yagishita · T. Takahashi · N. Amano
S. Murayama · S. Murakami · N. Shibata
M. Kobayashi · S. Sasaki · M. Iwata

Astrocytic plaques and tufts of abnormal fibers do not coexist in corticobasal degeneration and progressive supranuclear palsy

Received: 10 December 1997 / Revised, accepted: 23 March 1998

Abstract Corticobasal degeneration (CBD) and progressive supranuclear palsy (PSP) are characterized by their unique clinical features and neuronal pathology. Although astrocytic plaques and tufts of abnormal fibers have been suggested to be specific histopathologic markers, recent studies have revealed significant clinicopathologic overlap between CBD and PSP. Based on the distinctive camera lucida profile of astrocytic inclusions on Gallyas-Braak silver staining, we found that astrocytic plaques and tufts of abnormal fibers did not coexist in the same patient among 30 cases of clinically diagnosed CBD, PSP and atypical Parkinson's disease. Using Tau immunohistochemistry it was difficult to verify the absence of tufts of abnormal fibers. A morphometric analysis revealed that the two groups classified by the presence or absence of astrocytic plaques and tufts of abnormal fibers exhibited significant differences in the density of ballooned neurons and neurofibrillary tangles and degeneration of the subcortical nuclei. Assessment using the NINDS neuropathologic criteria revealed that the cases with astrocytic plaques and tufts of abnormal fibers closely correspond to CBD and typical PSP, respectively. In addition, the cases lacking either of these two astrocytic inclusions had atypical PSP according to the NINDS criteria, and were associated with novel tau-positive astrocytes (spiny astrocytes). We thus conclude that astrocytic plaques and tufts of abnormal fibers are highly characteristic structures for CBD and typical PSP, respectively. We emphasize the importance of strict differentiation between different astrocytic inclusions not only for diagnosis, but also for further studies for elucidation of their role in the disease mechanisms of CBD and PSP.

Key words Corticobasal degeneration · Progressive supranuclear palsy · Astrocytic plaques · Tufts of abnormal fibers · Gallyas-Braak silver staining

T. Komori (✉) · N. Arai
Department of Clinical Neuropathology,
Tokyo Metropolitan Institute for Neuroscience,
2-6 Musashidai, Fuchu City, Tokyo 183-8526, Japan
e-mail: komori@tmin.ac.jp,
Tel.: +81-423-25-3881, Fax: +81-423-21-8678

M. Oda · H. Nakayama · H. Mori
Department of Laboratory Medicine and Psychiatry,
Tokyo Metropolitan Neurological Hospital, Tokyo, Japan

S. Yagishita · T. Takahashi
Department of Pathology, Kanagawa Rehabilitation Center,
Yokohama, Japan

N. Amano · S. Murayama · S. Murakami
Department of Neuropsychiatry, Neurology and Pathology,
Faculty of Medicine, University of Tokyo, Tokyo, Japan

N. Shibata · M. Kobayashi · S. Sasaki · M. Iwata
Department of Pathology and Neurology,
Tokyo Women's Medical College, Tokyo, Japan

Introduction

Corticobasal degeneration (CBD) and progressive supranuclear palsy (PSP) are non-hereditary neurodegenerative disorders. CBD and PSP were originally characterized by their unique clinical features and neuronal pathology: preferential distribution of neuronal loss and the presence of ballooned neurons or neurofibrillary tangles (NFT) [18, 41, 43]. Although CBD and PSP have been considered to be distinct clinicopathologic entities, recent studies have revealed significant clinical and pathologic overlap between them. Both disorders are characterized by akinesia, rigidity, oculomotor abnormalities and late-onset dementia with marked variability between cases [3, 7, 9, 15, 17, 33, 39, 42, 44]. Pathologically, both can affect cortical and subcortical structures and they feature tau-immunoreactive neuronal and glial inclusions [12, 14, 15, 33, 45, 47, 48]. The neuronal inclusions in CBD have been termed corticobasal inclusions [18]. However, these neuronal inclusions have many features similar to globose NFTs in PSP: they are basophilic and tau positive, but not ubiquitin positive [13, 30]. Other studies have also demonstrated that ballooned neurons are present not only in CBD but also in PSP [21, 31, 34]. The oligodendroglial inclusions, which are referred to as coiled bodies, are

found in many neurodegenerative disorders including CBD, PSP and Alzheimer's disease [5, 22, 36, 46].

To date, three types of tau-positive, argyrophilic astrocytic inclusions have been identified in neurodegenerative disorders: astrocytic plaques [12, 25, 32], tufts of abnormal fibers [19, 40, 47] and thorn-shaped astrocytes [23]. Thorn-shaped astrocytes are known to be nonspecific [23, 35]; astrocytic plaques have been suggested to be specific for CBD, and tufts of abnormal fibers for PSP [1, 4, 8, 12, 14, 25], while one study suggested a close relationship between astrocytic plaques and tufts of abnormal fibers [37]. Thus, the precise morphologic differences between the two inclusions, and their actual specificities, particularly those of tufts of abnormal fibers for PSP, have not been determined.

In this study, using tau immunohistochemistry and Gallyas-Braak silver (GB) staining [6], we demonstrated the fine morphology of astrocytic inclusions and evaluated the specificity of astrocytic inclusions for CBD and PSP based on the quantitative analysis of neuronal pathology.

Materials and methods

Brains from a total of 30 autopsy cases (aged 55–86 years; 16 male, 14 female; mean age 73.0 years) who had been clinically diagnosed to have CBD, PSP and atypical Parkinson's disease were selected for analysis. Brains, obtained on autopsy, of 5 non-demented age-matched individuals who had not been diagnosed to have any neuropsychiatric disorders (age range, 64–88 years; mean 73.2 years), served as controls.

Tissues were obtained from multiple regions of the brains, fixed in 10% buffered formalin and paraffin-embedded. Sections, 10 μm thick, were cut, and stained by routine histochemical stainings, including hematoxylin and eosin (H&E), Bodian silver, Klüver-Barrera (KB) and Holzer stainings, as well as GB staining after pretreatment of sections with 0.3% $KMnO_4$, for identification of agyrophilic glia. Representative 5-μm-thick sections were immunostained using the streptavidin-biotin immunoperoxidase complex (ABC) method (Vector Laboratories, Burlingame, Calif.) with primary antibodies directed toward tau proteins (tau-1, monoclonal, 1:100, Boehringer Mannheim; tau-2, monoclonal, 1:500, Dako; and tau, polyclonal, 1:4000, Dako). Dephosphorylation was performed prior to tau-1 staining at 32°C for 2.5 h in a solution containing 100 nM TRIS-HCl pH 8.0, 130 U/ml alkaline phosphatase, 1 nM PMSF, 10 μg/ml pepstatin and 10 μg/ml leupeptin. Sections from which antibodies were omitted served as controls. Antibody binding was visualized using 3,3′-diaminobenzidine tetrahydrochloride as the final chromogen.

Using GB staining, the assessment of astrocytic inclusions was carried out in the cerebral cortex at the level of the mamillary body, putamen, caudate nucleus, amygdala and the tegmentum of the brain stem. A two-dimensional camera lucida profile of GB-positive astrocytes was drawn from five overlaid, 2-μm-interval step images of 10-μm-thick sections. For quantitative evaluation, ballooned neurons were counted on KB-stained sections from the convexity of the posterior frontal gyrus. Since corticobasal inclusions could not be satisfactorily distinguished from globose NFT, all the argyrophilic neuronal inclusions were counted as NFT. NFT were counted on Bodian-stained sections from the globus pallidus (GP), subthalamic nucleus (STN), cerebellar dentate nucleus (DTN) and substantia nigra (SN). Lewy bodies were counted on H&E-stained sections from the SN. The density of each inclusion in the targeted areas was calculated, using a computer-assisted image analysis system consisting of a microscope (Olympus BX 40), a CCD camera (KY-F55MD, Victor), a microcomputer (Power Macintosh 8500) and a software system (MacScope, Mitani, Fukui, Japan). In addition, the levels of degeneration of the subcortical nuclei were semiquantitatively scored from 0 (none) to 3 (severe) based on the degree of neuronal loss and gliosis using H&E and Holzer staining. All data were analyzed statistically using the Mann-Whitney's U test for effect grouping variable. A probability level of $P < 0.05$ was regarded as significant. Independent from the quantitative evaluation, the 30 cases studied were neuropathologically reevaluated using the preliminary pathologic criteria of the National Institute of Neurological Disorders and Stroke (NINDS) [20], which held a subtype category for PSP compared to the revised NINDS criteria [29].

Results

Morphologic characteristics of astrocytic inclusions

The results of tau immunohistochemistry and GB staining were compared. Astrocytic plaques were more clearly immunostained by tau-1 after dephosphorylation than by tau-2 and tau. They exhibited a corona-like arrangement and were composed of fuzzy short processes with tapering end and fine collaterals which were more evident on GB staining (Fig. 1 a, b). No cytoplasm staining was visualized within the astrocytic plaques. A spreading form of tau immunostaining was rarely identified except in one case. This spreading form did not reveal the fine collaterals of the astrocytic plaques and was not stained by GB. Within the same sections, adjacent to the astrocytic plaques, other tau-positive cells with astrocytic configuration were also detected. Some of them were confirmed to be astrocytes by means of their cell processes attached to the blood vessels (Fig. 1 c). While the appearance of astrocytic plaques on tau immunohistochemistry was similar to that on GB staining, the appearance of tufts of abnormal fibers on tau immunohistochemistry was markedly different from that on GB staining (Fig. 1 d, e). On tau immunohistochemistry, tufts of abnormal fibers exhibited a variety of appearances including occasional broad cytoplasmic staining (Fig. 1 e). They were more clearly immunostained by tau-2 and tau than by tau-1. On GB staining, they were observed as an aggregation of conglomerated, fine and thick processes with a concentric arrangement (Fig. 1 d). Some of the tufts also showed cytoplasmic processes attached to the blood vessels. On tau immunohistochemistry, some tufts could not be satisfactorily distinguished from tau-positive astrocytes in the sections containing astrocytic plaques. Independent of the inclusions mentioned, smaller tangle-like inclusions were detected with tau immunohistochemistry and GB staining. Some of them had fine processes terminating on the blood vessels and were confirmed to be astrocytic (spiny astrocytes) (Fig. 1 f).

The details of the differences between each astrocytic inclusion on GB staining were highlighted by camera lucida drawings (Fig. 2). The astrocytic plaques had short processes with fine collaterals at vertical or sharp angles, and tapering profiles at both ends. The collaterals were much thinner than the trunks (Fig. 2 a). The tufts of abnormal fibers exhibited tree-shaped branching without collat-

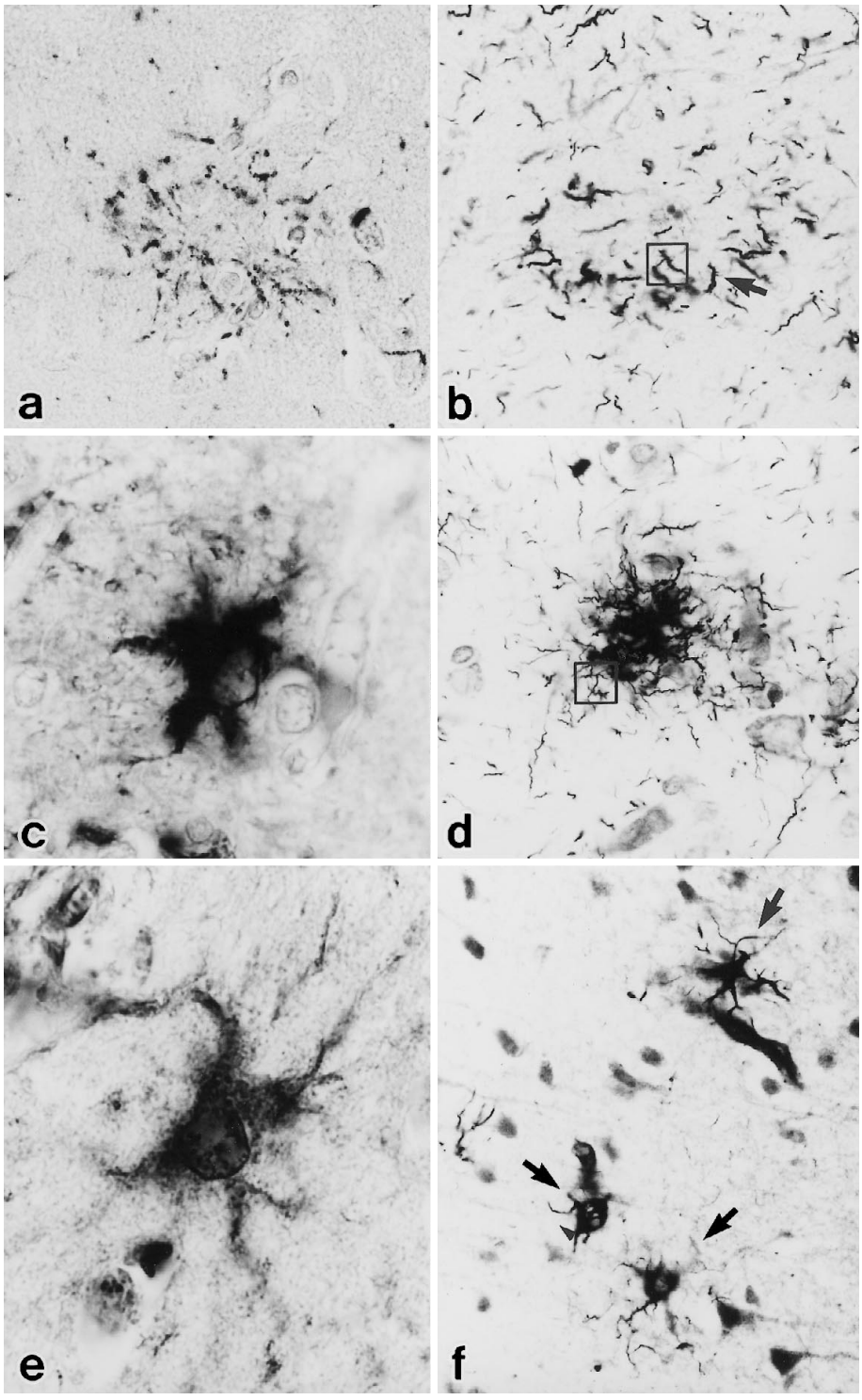

Fig. 1 a–f Astrocytic inclusions. Tau immunohistochemistry (**a**, **c**, **e**) and Gallyas-Braak silver staining (**b**, **d**, **f**). The *squares* indicate an approximately corresponding area in each camera lucida drawing (the drawing was obtained from a different section). **a**, **b** Astrocytic plaques. Note the fine collaterals (*arrow*). **c** Tau-positive astrocyte adjacent to astrocytic plaques. **d**, **e** Tufts of abnormal fibers. **f** Spiny astrocytes. **a**, **b**, **d**, **f** × 480; **c**, **e** × 960

erals. The branches exhibited a gradually decreasing caliber and blunt ends (Fig. 2 b). The spiny astrocyte had broad processes with a few fine branches and possessed a tangled appearance (Fig. 2 c). Although the cellular origin of not all of the GB-positive structures could be determined, at least the three types of astrocytic inclusions mentioned above were clearly distinguishable.

Subgroups divided by astrocytic inclusions

Based strictly on the morphologic characteristics on GB staining, it was noted that astrocytic plaques and tufts of abnormal fibers were not co-localized in the same case. The 30 cases could thus be divided into four subgroups: group I (10 cases) with astrocytic plaques, group II (13 cases) with tufts of abnormal fibers, group III (4 cases)

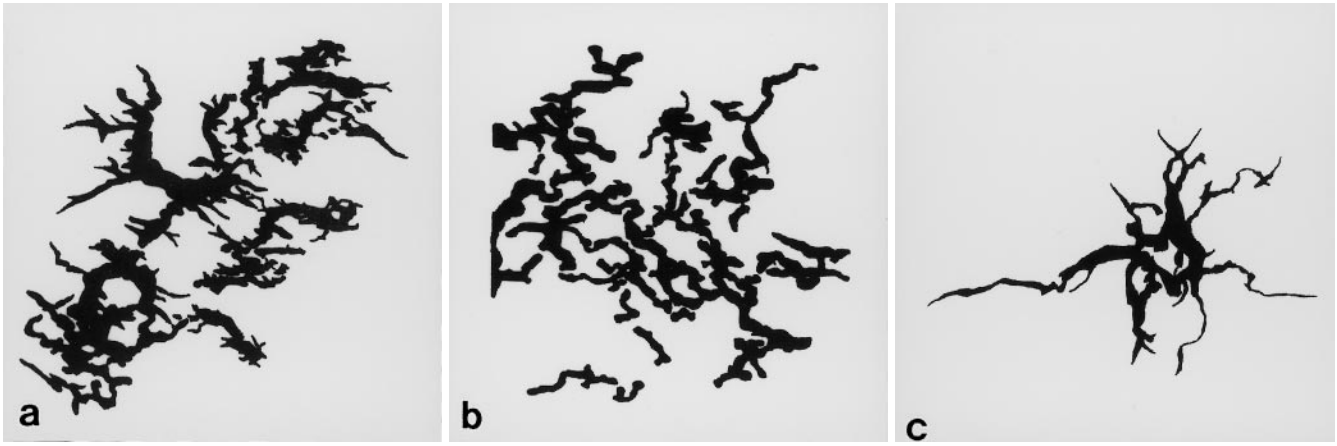

Fig. 2 a–c Camera lucida drawings of astrocytic inclusions with Gallyas-Braak silver staining. The differences in branching profiles are well demonstrated. **a** Astrocytic plaque. **b** Tufts of abnormal fibers. **c** Spiny astrocytes. **a**, **b** × 2010; **c** × 1710

lacking either astrocytic plaques or the tufts of abnormal fibers associated with spiny astrocytes, and group IV (3 cases) without any glial inclusions (Table 1). Occasional thorn-shaped astrocytes were identified in the subpial and subependymal zones in the control group and groups I–III. In the control cases, no plaques, tufts, or spiny astrocytes were detected.

Quantitative evaluation of neuronal pathology (Table 2)

Group I had high cortical ballooned neuron density and high NFT density and degeneration score in the SN. Group II exhibited high NFT density and degeneration score in all the areas studied. Group III showed results similar to those of group I, but had very low cortical ballooned neuron density. Group IV was characterized by the degeneration of the SN and high Lewy body density, but did not exhibit NFT or neuronal degeneration in the GP, STN and DTN.

Table 1 Subgroups classified by the type of astrocytic inclusions. Age is given as mean ± SD years (*M* male, *F* female, + present, – absent)

	Age, sex	Astrocytic inclusions			
		Astrocytic plaques	Tufts of abnormal fibers	Spiny astrocytes	Thorn-shaped astrocytes
Group I (*n* = 10)	69.4 ± 8.25 4M/6F	+	–	–	+
Group II (*n* = 13)	75.5 ± 4.72 8M/5F	–	+	–	+
Group III (*n* = 4)	75.5 ± 5.45 2M/2F	–	–	+	+
Group IV (*n* = 3)	71.0 ± 8.72 2M/1F	–	–	–	–

Table 2 Quantitative evaluation of neuronal pathology. The values represent the mean ± SD (*CRT* cerebral cortex, *GP* globus pallidus, *STN* subthalamic nucleus, *DTN* dentate nucleus, *SN* substantia nigra, *BN* ballooned neuron, *NFT* neurofibrillary tangles, *DGN* degeneration score, *LB* Lewy body)

	CRT	GP		STN		DTN		SN		
	BN/mm²	NFT/mm²	DGN	NFT/mm²	DGN	NFT/mm²	DGN	NFT/mm²	DGN	LB/mm²
Group I	0.29	0.17	1.17	1.78	1.20	0.24	0.58	0.72	2.17	0.0
	0.18	0.081	0.75	1.69	1.10	0.18	1.02	0.73	0.82	0.0
Group II	0.006	0.49	2.27	6.31	2.42	1.34	2.29	0.83	2.65	0.016
	0.012	0.25	0.56	4.95	0.57	1.12	0.78	0.33	0.43	0.058
Group III	0.009	0.165	1.25	2.92	1.75	0.46	1.0	0.76	2.63	0.075
	0.018	0.214	1.50	1.91	1.50	0.42	1.35	0.43	0.48	0.15
Group IV	0.002	0.0	0.0	0.04	0.0	0.02	0.0	0.0	2.33	0.72
	0.003	0.0	0.0	0.069	0.0	0.035	0.0	0.0	0.58	0.42

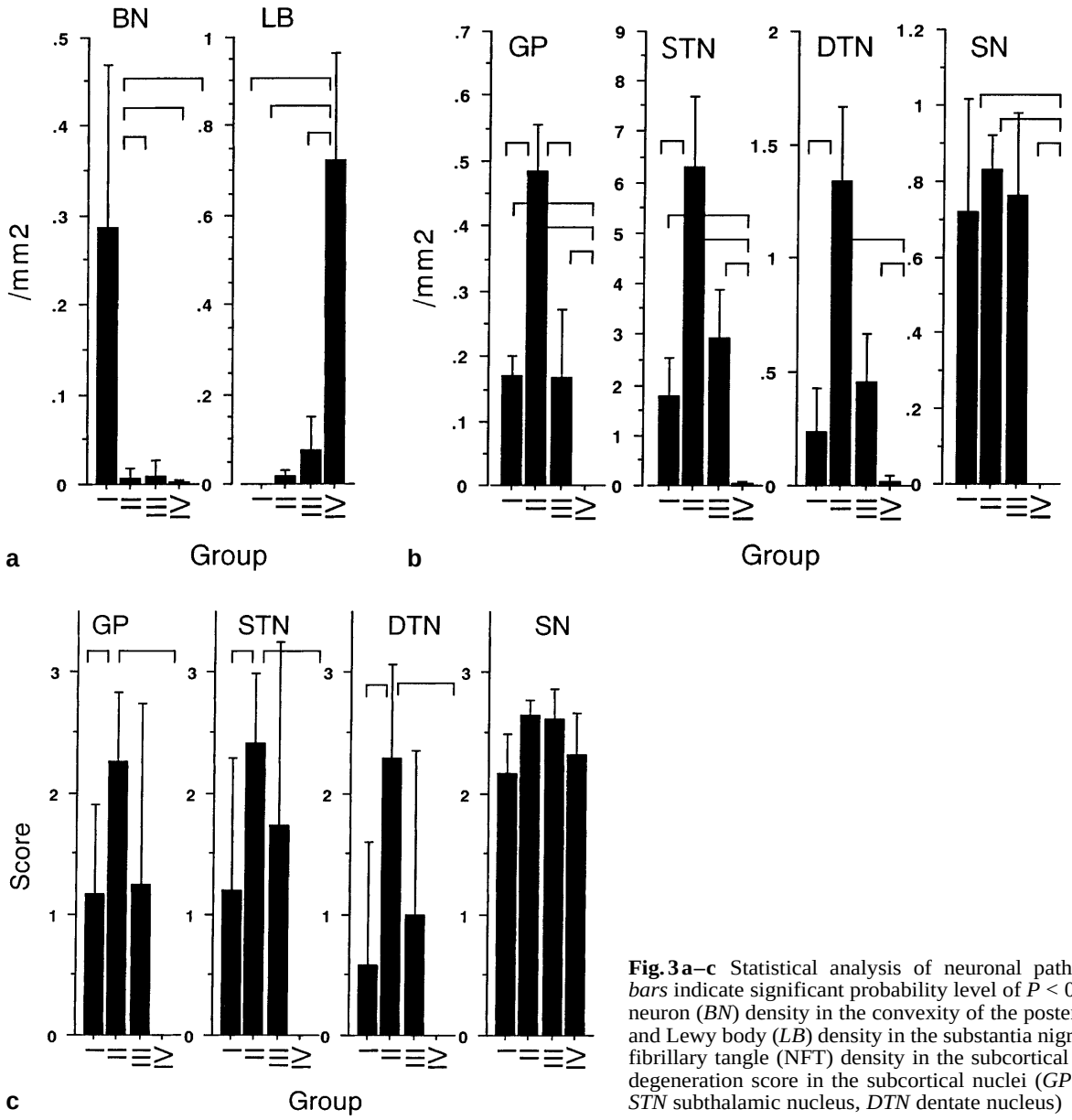

Fig. 3 a–c Statistical analysis of neuronal pathology. *Coupling bars* indicate significant probability level of $P < 0.05$. **a** Ballooned neuron (*BN*) density in the convexity of the posterior frontal gyrus and Lewy body (*LB*) density in the substantia nigra (SN). **b** Neurofibrillary tangle (NFT) density in the subcortical nuclei. **c** Neurodegeneration score in the subcortical nuclei (*GP* globus pallidus, *STN* subthalamic nucleus, *DTN* dentate nucleus)

Statistical analysis

Statistical analysis was performed between each subgroup, and no significant difference in patients' age was identified (Table 1). The density of cortical ballooned neurons was significantly higher in group I compared to the other groups (Fig. 3 a). Lewy body density was significantly higher in group IV compared to the other groups (Fig. 3 a). Significant differences between group I and II were observed for both NFT density and the degeneration score in the GP, STN and DTN (Fig. 3 b, c). In contrast, the only difference detected between group II and III was in NFT density in the GP (Fig. 3 b, c). Groups I, II and III had high NFT density and degeneration score in the SN, but no statistical difference was detected between the three groups (Fig. 3 b, c).

Clinical and pathologic diagnosis

The results of neuropathologic reevaluation based on the NINDS criteria are summarized in Table 3. All of the 10 cases in group I had a pathologic diagnosis of CBD (100%). Out of the 13 cases in group II, 12 had pathologically typical PSP (92%) and 1 had combined PSP (typical PSP but with Lewy bodies in the SN). All of the 4 cases in group III had atypical PSP and 2 of them had Lewy bodies in the SN. All of the 3 cases in group IV, without any glial inclusions, were found to have pathologic features compatible with Parkinson's disease. However, since the clinical diagnosis was PSP, no definitive pathologic diagnosis was made. All the cases of pathologically diagnosed as CBD had astrocytic plaques (100%). All of the 12 cases of typical PSP had tufts of abnormal fibers (100%), while out of 17 cases of PSP including the

Table 3 Clinical and pathologic diagnosis (*NINDS* National Institute of Neurological Disorders and Stroke, *ND* no definitive diagnosis)

	Clinical diagnosis	Pathologic diagnosis (NINDS, 1994)
Group I (n = 10)	7 CBD/ 3 PSP	10 CBD
Group II (n = 13)	1 CBD/ 10 PSP/ 2 atypical PD	12 typical PSP/ 1 combined, typical PSP
Group III (n = 4)	1 PSP/ 3 atypical PD	2 atypical PSP/ 2 combined, atypical PSP
Group IV (n = 3)	3 PSP	3 ND

combined and atypical cases, 13 had tufts of abnormal fibers (76%). Thus, in our study, the specificity of astrocytic plaques for pathologic CBD was 100% and that of tufts of abnormal fibers for pathologically typical PSP was 92%. The sensitivity of astrocytic plaques as an indication for CBD was 100% and that for tufts of abnormal fibers was 100% for typical PSP, while it was only 76% when the combined and atypical PSP cases were also considered.

Discussion

Based on the distinctive morphologic profiles of astrocytic inclusions, we observed that astrocytic plaques and tufts of abnormal fibers essentially do not co-exist. The two groups classified by the presence or absence of astrocytic plaques and tufts of abnormal fibers exhibited significant differences in neuronal pathology such as a difference in the density of ballooned neurons, NFT and degeneration of the subcortical nuclei. The pathologic features of these two groups corresponded well to the features of CBD and typical PSP as outlined in the preliminary NINDS criteria [20]. Specificity and sensitivity of astrocytic plaques for CBD were 100% and those for tufts of abnormal fibers for typical PSP were more than 90%. All things considered, we concluded that astrocytic plaques and tufts of abnormal fibers are highly characteristic features of CBD and typical PSP. However, 3 of the 10 cases in group I had a clinical diagnosis of PSP, while 1 of 13 cases in group II had a clinical diagnosis of CBD. This result is in agreement with previous reports that CBD and PSP can be clinically overlapped [3, 7, 9, 15, 17, 33, 39, 42, 44]. Our study also confirmed the presence of ballooned neurons in PSP as previously described [15, 21, 31, 34], but revealed that their density in CBD was more than 30 times greater than in PSP. Thus, the presence of ballooned neurons is a reliable marker for CBD as described in a previous semiquantitative study [15]. In contrast, our study suggested that NFT pathology in CBD and PSP was essentially identical; both have similar preferential targets, GP, STN, DTN and SN. Although the overall NFT density is higher and DTN is more severely affected in PSP than in CBD, it may be difficult to distinguish between individual cases of PSP or CBD only on the basis of NFT pathology. Therefore, the presence of specific astrocytic inclusions may be highly reliable histopathologic markers for CBD and PSP.

The nosologic position of group III, which lacked tufts of abnormal fibers but had spiny astrocytes, remains unclear. Group III had an overall low NFT density and degeneration score in the subcortical nuclei and corresponded to atypical or combined PSP based on the NINDS criteria [20], although the NFT density in the GP was significantly lower compared to group II (typical PSP group). In addition, three of the four cases of group III had a clinical diagnosis of atypical Parkinson's disease and two showed Lewy bodies in the SN. In the revised NINDS criteria, atypical PSP was excluded as a PSP subtype, and combined PSP was restricted to the cases with coexistence of infarcts but not Lewy bodies [29]. However, the combined PSP cases in our study with a small number of Lewy bodies in the SN cannot be classified as Parkinson's disease, since Lewy bodies are found in a variety of neurologic diseases [30] and developed with aging [16]. Further studies on atypical PSP are needed to establish its nosologic position in the spectrum of parkinsonian syndrome.

In addition to the astrocytic inclusions, we previously demonstrated that cortical neuropil threads in CBD and PSP were morphologically and morphometrically different; the neuropil threads in PSP were long and wide, and more parallel than those in CBD [27]. Their density was highest in the cerebral cortical layer V in CBD, and in the subcortical white matter in PSP [27]. Such a difference in the laminar distribution of neuropil threads between CBD and PSP has also been demonstrated by others [4, 10, 13, 19]. These differences might be explained by differences either in cellular localization, ultrastructural profiles or by as yet unidentified factors [27]. We and others have previously demonstrated that at least a portion of the cortical neuropil threads in PSP are formed from the processes of oligodendrocytes [2, 26].

Immunohistochemically, neuronal and glial cytoskeletal lesions in both CBD and PSP are known to contain hyperphosphorylated tau epitopes [14, 22]. An antibody against tau, the genes for which contain an alternatively spliced exon 3, did not recognize cytoskeletal lesions in CBD but recognized NFT and neuropil threads in PSP [14]. Another study, however, has reported that this antibody recognized neuronal cytoskeletal lesions in both CBD and PSP, but failed to recognize any of the glial inclusions in either CBD or PSP [38]. Thus, tau immunohistochemistry has not succeeded in unequivocally distinguishing between different astrocytic inclusions. Our study has shown that GB staining is better than tau immunohistochemistry for the demonstration of astrocytic inclusions. While GB staining highlights the distinctive morphology of inclusions, tau immunohistochemistry did not permit subclassification of astrocytic inclusions, particularly because of the difficulty in verifying the absence of tufts of abnormal fibers. A spreading form of tau-positive astrocytic plaques has been described in CBD [14], but we found that this form is GB negative and rarely

identified in CBD. The relationship of this form to GB-positive astrocytic plaques remains unclear.

GB staining sensitively detects not only abnormal tau but also high-molecular-weight microtubule-associated polypeptides [24]. Biochemically, tau in both CBD and PSP is composed of a doublet of 64 and 68 kDa [11, 28]. It is not known whether the doublet of CBD and PSP is identical, but one study has demonstrated that the tau of CBD was more acidic than that of PSP in a two-dimensional gel analysis [11]. It is also unknown whether this subtle biochemical difference depends on neuronal abnormality, glial abnormality or both.

Although the fundamental pathologic mechanisms underlying CBD and PSP remain unknown, the distinct morphology of astrocytic inclusions and neuropil threads in CBD and PSP may reflect a particular mode of assembly of tau, which may or may not be regulated by an unknown gene abnormality. Thus, a morphologic study would not only aid diagnosis, but also the elucidation of the underlying pathomechanisms. Furthermore, the existence of differences in the expression of tau leads one to argue against the view that tau expression is only a secondary phenomenon occurring subsequent to neuronal degeneration of undetermined cause.

In conclusion, we emphasize the importance of the strict differentiation between astrocytic inclusions using GB staining in CBD, PSP and their related disorders, since, first, the pathologic phenotype as classified by the morphology of astrocytic inclusions are well correlated with neuronal pathology; second, the detection of astrocyte pathology may be more specific and sensitive than neuronal pathology; and third, the distinctive differences between astrocytes may reflect discrete underlying pathomechanisms including the genetic basis. Further studies should focus on astrocyte pathology to elucidate the role of astrocytes in the disease mechanisms of CBD and PSP.

Acknowledgements The technical assistance of Ms. Reiko Umizu is gratefully acknowledged. This study was supported by a research grant from the Tokyo Metropolitan Government.

References

1. Arai N (1996) A variety of glial pathological structures by the modified Gallyas-Braak method. Neuropathology 16:133–138
2. Arima K, Nakamura M, Sunohara N, Ogawa M, Anno M, Izumiyama Y, Horai S, Ikeda K (1997) Ultrastructural characterization of the tau-immunoreactive tubules in the oligodendroglial perikarya and their inner loop processes in progressive supuranuclear palsy. Acta Neuropathol 93:558–566
3. Bergeron C, Pollanen MS, Weyer L, Black SE, Lang AE (1996) Unusual clinical presentations of cortical-basal ganglionic degeneration. Ann Neurol 40:893–900
4. Bergeron C, Pollanen MS, Weyer L, Lang AE (1997) Cortical degeneration in progressive supranuclear palsy. A comparison with cortical-basal ganglionic degeneration. J Neuropathol Exp Neurol 56:726–734
5. Braak H, Braak E (1989) Cortical and subcortical argyrophilic grains characterize a disease associated with adult onset dementia. Neuropathol Appl Neurobiol 15:13–26
6. Braak H, Braak E, Ohm T, Bohl J (1988) Silver impregnation of Alzheimer's neurofibrillary changes counterstained for basophilic material and lipofuscin pigment. Stain Technol 63:197–200
7. Capitani E, Laiacona M, Barbarotto R (1993) Progressive neuropsychological and extrapyramidal deterioration resembling progressive supranuclear palsy: is aphasia relevant for correct diagnosis? Eur Arch Psychiatry Clin Neurosci 242:347–351
8. Chin SS, Goldman JE (1996) Glial inclusions in CNS degenerative diseases. J Neuropathol Exp Neurol 55:499–508
9. Collins SJ, Ahlskog JE, Parisi JE, Maraganore DM (1995) Progressive supranuclear palsy: neuropathologically based diagnostic clinical criteria. J Neurol Neurosurg Psychiatry 58:167–173
10. Davis DG, Wang HZ, Markesbery WR (1992) Image analysis of neuropil threads in Alzheimer's, Pick's, diffuse Lewy body disease and in progressive supranuclear palsy. J Neuropathol Exp Neurol 51:594–600
11. Delacourte A, Robitaille Y, Sergeant N, Buee L, Hof PR, Wattez A, Larochecholette A, Mathieu J, Chagnon P, Gauvreau D (1996) Specific pathological tau protein variants characterize Pick's disease. J Neuropathol Exp Neurol 55:159–168
12. Feany MB, Dickson DW (1995) Widespread cytoskeletal pathology characterizes corticobasal degeneration. Am J Pathol 146:1388–1396
13. Feany MB, Dickson DW (1996) Neurodegenerative disorders with extensive tau pathology: a comparative study and review. Ann Neurol 40:139–148
14. Feany MB, Ksiezakreding H, Liu WK, Vincent I, Yen SHC, Dickson DW (1995) Epitope expression and hyperphosphorylation of tau protein in corticobasal degeneration – Differentiation from progressive supranuclear palsy. Acta Neuropathol 90:37–43
15. Feany MB, Mattiace LA, Dickson DW (1996) Neuropathologic overlap of progressive supranuclear palsy, Pick's disease and corticobasal degeneration. J Neuropathol Exp Neurol 55:53–67
16. Forno L (1969) Concentric hyalin intraneuronal inclusions of Lewy type in the brains of elderly persons (50 incidental cases). J Am Geriatr Soc 17:557–575
17. Gearing M, Olson DA, Watts RL, Mirra SS (1994) Progressive supranuclear palsy: neuropathologic and clinical heterogeneity. Neurology 44:1015–1024
18. Gibb W, Luthert P, Marsden C (1989) Corticobasal degeneration. Brain 112:1171–1192
19. Hauw JJ, Verny M, Delaere P, Cervera P, He Y, Duyckaerts C (1990) Constant neurofibrillary changes in the neocortex in progressive supranuclear palsy. Basic differences with Alzheimer's disease and aging. Neurosci Lett 119:182–186
20. Hauw JJ, Daniel SE, Dickson D, Horoupian DS, Jellinger K, Lantos PL, McKee A, Tabaton M, Litvan I (1994) Preliminary NINDS neuropathologic criteria for Steele-Richardson-Olszewski syndrome (progressive supranuclear palsy). Neurology 44:2015–2019
21. Higuchi Y, Iwaki T, Tateishi J (1995) Neurodegeneration in the limbic and paralimbic system in progressive supranuclear palsy. Neuropathol Appl Neurobiol 21:246–254
22. Ikeda K, Akiyama H, Haga C, Kondo H, Arima K, Oda T (1994) Argyrophilic thread-like structure in corticobasal degeneration and supranuclear palsy. Neurosci Lett 174:157–159
23. Ikeda K, Akiyama H, Kondo H, Haga C, Tanno E, Tokuda T, Ikeda S (1995) Thorn-shaped astrocytes – possibly secondarily induced tau-positive glial fibrillary tangles. Acta Neuropathol 90:620–625
24. Iqbal K, Braak E, Braak H, Zaidi T, Grundke Iqbal I (1991) A silver impregnation method for labeling both Alzheimer paired helical filaments and their polypeptides separated by sodium dodecyl sulfate-polyacrylamide gel electrophoresis. Neurobiol Aging 12:357–361
25. Komori T, Shibata N, Kobayashi M (1995) Plaque-like structures in the cerebral cortex of corticobasal degeneration: a histopathologic marker? Neuropathology 15:175–176

26. Komori T, Shibata N, Kobayashi M, Sasaki S (1995) Argyrophilic meshwork structures in the cerebral cortex of patients with progressive supranuclear palsy. Neuropathology 16 : 1–5
27. Komori T, Arai N, Oda M, Nakayama H, Murayama S, Amano N, Shibata N, Kobayashi M, Sasaki S (1997) Morphologic difference of neuropil threads in Alzheimer's disease, corticobasal degeneration and progressive supranuclear palsy: a morphometric study. Neurosci Lett 233 : 89–92
28. Ksiezakreding H, Tracz E, Yang LS, Dickson DW, Simon M, Wall JS (1996) Ultrastructural instability of paired helical filaments from corticobasal degeneration as examined by scanning transmission electron microscopy. Am J Pathol 149 : 639–651
29. Litvan I, Hauw JJ, Bartko JJ, Lantos PL, Daniel SE, Horoupian DS, McKee A, Dickson D, Bancher C, Tabaton M, Jellinger K, Anderson DW (1996) Validity and reliability of the preliminary NINDS neuropathologic criteria for progressive supranuclear palsy and related disorders. J Neuropathol Exp Neurol 55 : 97–105
30. Lowe J, Lennox G, Leigh PN (1997) Disorders of movement and system degenerations. In: Graham D, Lantos P (eds) Greenfield's neuropathology. Arnold, London, pp 261–366
31. Mackenzie IR, Hudson LP (1995) Achromatic neurons in the cortex of progressive supranuclear palsy. Acta Neuropathol 90 : 615–619
32. Mattiace L, Wu E, Aronson M, Dickson D (1991) A new type of neuritic plaque without amyloid in corticonigral degeneration with neuronal achromasia (abstract). J Neuropathol Exp Neurol 50 : 310
33. Mori H, Nishimura M, Namba Y, Oda M (1994) Corticobasal degeneration: a disease with widespread appearance of abnormal tau and neurofibrillary tangles, and its relation to progressive supranuclear palsy. Acta Neuropathol 88 : 113–121
34. Mori H, Oda M, Mizuno Y (1996) Cortical ballooned neurons in progressive supranuclear palsy. Neurosci Lett 209 : 109–112
35. Nishimura M, Namba Y, Ikeda K, Oda M (1992) Glial fibrillary tangles with straight tubules in the brains of patients with progressive supranuclear palsy. Neurosci Lett 143 : 35–38
36. Nishimura M, Tomimoto H, Suenaga T, Namba Y, Ikeda K, Akiguchi I, Kimura J (1995) Immunocytochemical characterization of glial fibrillary tangles in Alzheimer's disease brain. Am J Pathol 146 : 1052–1058
37. Nishimura T, Ikeda K, Akiyama H, Kondo H, Kato M, Li F, Iseki E, Kosaka K (1995) Immunohistochemical investigation of tau-positive structures in the cerebral cortex of patients with progressive supranuclear palsy. Neurosci Lett 201 : 123–126
38. Nishimura T, Ikeda K, Akiyama H, Arai T, Kondo H, Okochi M, Furiya Y, Mori H, Oda T, Kato M, Iseki E (1997) Glial tau-positive structures lack the sequence encoded by exon 3 of the tau protein gene. Neurosci Lett 224 : 169–172
39. Pillon B, Blin J, Vidailhet M, Deweer B, Sirigu A, Dubois B, Agid Y (1995) The neuropsychological pattern of corticobasal degeneration: comparison with progressive supranuclear palsy and Alzheimer's disease. Neurology 45 : 1477–1483
40. Probst A, Langui D, Lautenschlager C, Ulrich J, Brion JP, Anderton BH (1988) Progressive supranuclear palsy: extensive neuropil threads in addition to neurofibrillary tangles. Very similar antigenicity of subcortical neuronal pathology in progressive supranuclear palsy and Alzheimer's disease. Acta Neuropathol 77 : 61–68
41. Rebeiz J, Kolodny E, Richardson E (1968) Corticodentatonigral degeneration with neuronal achromasia. Arch Neurol 18 : 20–33
42. Savoiardo M, Girotti F, Strada L, Ciceri E (1994) Magnetic resonance imaging in progressive supranuclear palsy and other parkinsonian disorders. J Neural Transm [Suppl] 42 : 93–110
43. Steele JC, Richardson JC, Olszewski J (1964) Progressive supranuclear palsy. Arch Neurol 10 : 333–359
44. Verny M, Jellinger KA, Hauw JJ, Bancher C, Litvan I, Agid Y (1996) Progressive supranuclear palsy – a clinicopathological study of 21 cases. Acta Neuropathol 91 : 427–431
45. Wakabayashi K, Oyanagi K, Makifuchi T, Ikuta F, Homma A, Homma Y, Horikawa Y, Tokiguchi S (1994) Corticobasal degeneration: etiopathological significance of the cytoskeletal alterations. Acta Neuropathol 87 : 545–553
46. Yamada T, McGeer PL (1990) Oligodendroglial microtubular masses: an abnormality observed in some human neurodegenerative diseases. Neurosci Lett 120 : 163–166
47. Yamada T, McGeer PL, McGeer EG (1992) Appearance of paired nucleated, tau-positive glia in patients with progressive supranuclear palsy brain tissue. Neurosci Lett 135 : 99–102
48. Yamada T, Calne DB, Akiyama H, McGeer EG, McGeer PL (1993) Further observations on tau-positive glia in the brains with progressive supranuclear palsy. Acta Neuropathol 85 : 308–315